A mathematical model to compute the thermally affected zone at laser beam processing

M. PEARSICĂ, S. BĂLUȚĂ[a], C. CONSTANTINESCU, S. NEDELCU, C. STRÎMBU, M. D. BENȚA[b]
"Henri Coandă" Air Force Academy, IT and Electronic Department, 160 Mihai Viteazu St, 500183 Brasov, Romania
[a]*The Military Equipment and Technologies Research Agency, 16 Aeroportului St, OP Bragadiru, 077025, Ilfov, Romania*
[b]"Transilvania" University, 29 Eroilor St, 500036 Brasov, *Romania*

The study of thermic affected zone assumes determination of radial temperature distribution for large processing periods. This approach deals with a method to determine the thermally affected zone dimensions (area of melted and solidified material), concerning the metals processing using a power laser beam assisted by an active gas jet (O_2). Spatially and temporally distribution of temperature inside the material is governed by the full temperature source, which has been modelled by taking into consideration the fact that the irradiation is made with a laser with "Gaussian distribution" of photons beam's intensity and oxidization energy. The results thus obtained allow determining the technological parameters of processing and the material constants. The theoretical results obtained by using the proposed method were confirmed by the experimental ones.

(Received July 14, 2009; accepted January 19, 2010)

Keywords: Laser, Thermal affected zone, Temperature distribution

1. Introduction

Laser beam processing [1,11,13] is mainly a thermic one, material drawing being the consequence of two physical phenomena: melting and vaporization. Laser beam energy in the interaction moment will be reflected and partially absorbed by the material, a strong heating of the irradiated zone appearing in this way. The material thermal conductibility has a decisive role in this process, being increased by the presence of an assisting gas. The thermic affected zone is approximated by the material domain of melting, followed by a solidifying [6,9]. Thermally affected zone study requires computing the radial temperature distribution in material for large irradiation periods.

The time evolution of the temperature distribution into a system is strictly related to the appearance of the heat flux from the hottest regions to the coldest ones. A good approximation of the thermal effects involved during laser beam – processed material of the surface is offered by the thermal equation [3,4,5], which relates the absorbed energy flow and the material temperature. The invariant form of the thermal equation for an isotropic medium is given by (1).

$$\frac{\rho \cdot c_v}{k}\frac{\partial T}{\partial t} = \Delta T \tag{1}$$

where: $\rho[kg/m^3]$ is the mass density; $c_v[J \cdot kg^{-1} \cdot K^{-1}]$ – volumetric specific heat; $T[K]$ – temperature; $k[W \cdot m^{-1} \cdot K^{-1}]$ – thermal conductivity of the material; $t[s]$ – time; Δ – Laplace operator.

Because the imprint of the laser beam on the material surface is a circular one, thermal phenomena produced within the substantial, have a cylindrical symmetry. Here Oz is considered as symmetry axis of the laser beam, the object surface equation is $z = 0$ and the positive sense of Oz axis is from the surface to the inside of the object.

The thermal equation within cylindrical co-ordinates (θ, r, z) will be:

$$\frac{1}{K}\frac{\partial T}{\partial t} = \frac{1}{r^2}\frac{\partial^2 T}{\partial \theta^2} + \frac{1}{r}\frac{\partial}{\partial r}\left(r\frac{\partial T}{\partial r}\right) + \frac{\partial^2 T}{\partial z^2} \tag{2}$$

where: $K[m^2/s]$ is the diffusivity of the material.

Due to cylindrical symmetry, $\frac{\partial^2 T}{\partial \theta^2} = 0$ and equation (2) changes into:

$$\frac{1}{K}\frac{\partial T}{\partial t} = \frac{1}{r}\frac{\partial T}{\partial r} + \frac{\partial^2 T}{\partial r^2} + \frac{\partial^2 T}{\partial z^2} \tag{3}$$

Limit and oneness conditions are attached to thermal equation according to the particularly cases which are the discussed subject [3,4,9]. These conditions are time and space dependent.

If d is the laser beam radius and the origin of the coordinates is on its the beam symmetry axis, then the thermic flow imposed on the material surface (Neumann type condition) is given by [3,8]:

$$\left.\frac{\partial T}{\partial x}\right|_{z=0} = \begin{cases} -\frac{1}{k}\varphi_S(M,t), & x^2 + y^2 \le d^2,\ z = 0 \\ 0, & x^2 + y^2 > d^2,\ z = 0 \end{cases} \tag{4}$$

where $\varphi_S(M,t)$ is the power flow on the processed surface.

2. Temperature source modeling

The destruction of the crystalline network of the material and its vaporization, along the pre-established curve, is completed by the energy of photons created inside the material, and by the jet of the assisting gas (O_2). This gas intensifies the material destroying action due to the exothermal reactions provided.

The irradiated area being much smaller than the size of the object, the pattern D dealing with thermal equation may be approached as a semi-space.

Dealing with a semi-infinite solid heated by a laser beam uniform absorbed in its volume, it is assumed that Beer law governs its absorption at z depth. It is considered a radial "Gaussian" distribution of the laser beam intensity, which corresponds to the central part of the laser beam. It results the photons distribution in material volume:

$$I(r,z) = I_o \, e^{-\left[\left(\frac{r}{d}\right)^2 + \frac{z}{l}\right]} \tag{5}$$

where: I_o is the photons fascicule intensity on the material surface, and l is the attenuation length of laser radiation. I_o results as:

$$I_o = \frac{P_L}{h\nu \cdot \pi d^2} \tag{6}$$

where: P_L is the laser power; πd^2 – irradiated surface, and $h\nu$ is the energy of one photon.

It is assumed that photons energy is totally transformed in heat. So, the heat increasing rate, owing the photons energy, at z depth (under surface) is given by:

$$\frac{dQ}{dt \cdot dV} = h\nu \cdot \sigma \cdot \rho \cdot I(r,z) = \frac{P_L}{\pi d^2 \cdot l} e^{-\left[\left(\frac{r}{d}\right)^2 + \frac{z}{l}\right]} \tag{7}$$

where: dV and dt are the infinitesimal volume and time respectively, σ – the absorption cross section, $\sigma = 1/\rho \cdot l$.

The vaporized material diffuses in oxygen atmosphere and oxidizes exothermally, resulting in this way an oxidation energy, which appears as an additional kinetic energy of the surface gas constituents, leading to an additional heating of the laser processed zone. The rate of oxidizing energy release [7] on the material surface is given by (8):

$$\frac{dQ_{ox}}{dt \cdot dV} = \eta_o \cdot \varepsilon \cdot \sigma_{ox} \cdot n_{o_2} \cdot \bar{v}_M \cdot n_M \tag{8}$$

where: η_o is the oxidizing efficiency, ε – oxidizing energy on completely oxidized metal atom; σ_{ox} – effective oxidizing section; n_{o_2} – oxygen atomic concentration; $\bar{v}_M$ – average speed of vaporized metal atoms; n_M – atomic concentration of the unoxidized metal vapors.

The mass conservers itself, so the following relation results for the flow of vaporized atoms:

$$n_M \cdot \bar{v}_M = \frac{\rho}{M} v_s \tag{9}$$

where $v_s[m/s]$ is the vaporization boundary speed, and M is the atomic mass of the metal. It is assumed an exponential attenuation of the metal vapors flow and oxidizing is only inner laser irradiated zone, the oxidizing energy having a "Gaussian" distribution. The rate of oxidation energy release is given by:

$$\frac{dQ_{ox}}{dt \cdot dV} = \eta_o \cdot \sigma_{ox} \cdot \rho \cdot n_{o_2} \cdot v_s \frac{\varepsilon}{M} e^{\left[\frac{z}{l_{ox}} - \left(\frac{r}{d}\right)^2\right]} \tag{10}$$

where: l_{ox} is the oxidation length $[l_{ox} = 1/(n_{o_2} \cdot \sigma_{ox})]$; $\sigma_{ox} = \pi r_o^2$ (r_o – O_2 molecular radius, which may be considered $\approx 1A$). In (10), z is negative outside the material, so the attenuation is obvious.

The full temperature source results as a sum of (7) and (10):

$$S(r,z) = e^{-\left(\frac{r}{d}\right)^2} \cdot \left[\frac{P_L}{\pi d^2 \cdot l} e^{-\frac{z}{l}} \cdot h(z) + \eta_o \frac{\varepsilon \cdot \rho \cdot v_s}{M \cdot l_{ox}} e^{\frac{z}{l_{ox}}} \cdot h(-z)\right] \tag{11}$$

where h(x) is Heaviside function.

In temperature source expression, z origin is the same with the vaporization boundary, which advances in depth as the material is drawn.

Assuming a constant vaporization boundary speed, v_s, the instantaneous expression of the temperature source is given by:

$$S(r,z,t) = e^{-\left(\frac{r}{d}\right)^2} \left[\frac{P_L}{\pi d^2 \cdot l} e^{-\frac{z - v_s \cdot t}{l}} \cdot h(z - v_s \cdot t) + \eta_o \frac{\varepsilon \cdot \rho \cdot v_s}{M \cdot l_{ox}} e^{-\frac{v_s \cdot t - z}{l_{ox}}} \cdot h(v_s \cdot t - z)\right] \tag{12}$$

The spatial and temporal temperature distribution in material is governed by the full temperature source and results by solving the thermal equation.

3. Computing temperature analytical distribution

If one takes into account the expression of full the temperature source, temperature distribution is given by:

$$T(r,z,t) = T_a + T_1(r,z,t) + T_2(r,z,t) \tag{13}$$

where T_a is the environment temperature at the initial moment, and T_1 and T_2 are the contributions of laser ang assisting gas, respectively. According to a "Gaussian" distribution of the energy source, considered on the boundary of a halfi-space, the of the solution is given by [3,4]:

$$T(r,z,t)=\frac{\varphi_o\cdot d^2}{k_T}\left(\frac{K}{\pi}\right)^{\frac{1}{2}}\int_0^t\frac{e^{\left(-\frac{z^2}{4K\xi}-\frac{r^2}{4K\xi+d^2}\right)}}{\sqrt{\xi}\left(4K\xi+d^2\right)}d\xi \qquad (14)$$

where φ_o is the maximum power flow in the middle of material.

In the particularly case of the full temperature source given by (12) and respecting the "Gaussian" distribution of photons beam intensity and oxidation energy as boundary condition corresponding to the related semi-space, temperatures T_1 and T_2 are the following:

$$T_1(r,z,t)=\frac{P_L}{\pi^{3/2}\cdot\rho\cdot c\cdot\sqrt{K}}\int_0^t\frac{e^{-\left[\frac{r^2}{4v_{T1}\cdot l\cdot\xi+d^2}+\frac{(z-v_s\cdot\xi)^2}{4v_{T1}\cdot l\cdot\xi}\right]}}{\sqrt{\xi}\left(4v_{T1}\cdot l\cdot\xi+d^2\right)}d\xi$$

$$T_2(r,z,t)=\eta_o\frac{\varepsilon\cdot\rho\cdot v_s\cdot d^2}{\sqrt{\pi}\cdot M\cdot\rho\cdot c\cdot\sqrt{K}}\int_0^t\frac{e^{-\left[\frac{r^2}{4v_{T2}\cdot l_{ox}\cdot\xi+d^2}+\frac{(z-v_s\cdot\xi)^2}{4v_{T2}\cdot l_{ox}\cdot\xi}\right]}}{\sqrt{\xi}\left(4v_{T2}\cdot l_{ox}\cdot\xi+d^2\right)}d\xi \qquad (15)$$

where v_{T1} and v_{T2} are the speeds of thermal conduction:

$$v_{T1}=K/l,\ \ v_{T2}=K/l_{ox}\Rightarrow K=v_{T1}\cdot l=v_{T2}\cdot l_{ox} \qquad (16)$$

By replacing (15) and (16) in (13) it results:

$$T(r,z,t)=T_a+\left(\frac{P_L}{\pi}+\eta_o\frac{\varepsilon\cdot\rho\cdot v_s\cdot d^2}{M}\right)\frac{1}{\sqrt{\pi K}\cdot\rho\cdot c}\int_0^t\frac{e^{-\left[\frac{r^2}{4K\xi+d^2}+\frac{(z-v_s\cdot\xi)^2}{4K\xi}\right]}}{\sqrt{\xi}\left(4K\xi+d^2\right)}d\xi \qquad (17)$$

The expression (17) describes the temperature field corresponding to extended irradiation periods as an increasing function, followed by saturation. It results that vaporization boundary acts as a temperature wave, increasing its intensity till saturation. Assuming extended irradiation periods, it may be observed that isotherms are spheres centered on vaporization boundary ($z=v_s\cdot t$).

With $z=v_s\cdot t$ and dimensionless variable $y=2\sqrt{K\xi}/d$ in (17), the temperature distribution nearby the vaporization boundary results as it follows:

$$T(r,t)=T_a+\left(\frac{P_L}{\pi}+\eta_o\frac{\varepsilon\cdot\rho\cdot v_s\cdot d^2}{M}\right)\frac{1}{\sqrt{\pi}K\cdot\rho\cdot c\cdot d}\int_0^{\frac{2\sqrt{Kt}}{d}}\frac{e^{-\frac{r^2}{d^2\left(1+y^2\right)}}}{1+y^2}dy \qquad (18)$$

If the irradiation period is very large, the temperature increases. So, in (18), for $t\to\infty$ yields:

$$T_{max}=T_a+\left(\frac{P_L}{\pi}+\eta_o\frac{\varepsilon\cdot\rho\cdot v_s\cdot d^2}{M}\right)\frac{\sqrt{\pi}}{2\cdot k\cdot d} \qquad (19)$$

It results that maximum temperatures owed to laser and assisting gas contributions (T_{1max} and T_{2max} respectively) are given by:

$$T_{1max}=\frac{P_L}{2\sqrt{\pi}\cdot k\cdot d};\quad T_{2max}=\eta_o\frac{\sqrt{\pi}\varepsilon\cdot v_s\cdot\rho\cdot d}{2\cdot k\cdot M} \qquad (20)$$

By replacing (20) in (18) it results a simplified expression of radial temperature distribution, nearby the vaporization boundary:

$$T(r,t)=T_a+\left(T_{1max}+T_{2max}\right)\cdot F_d(r,t) \qquad (21)$$

where the following notation was used:

$$F_d(r,t)=\frac{2}{\pi}\int_0^{\frac{2\sqrt{Kt}}{d}}\frac{\exp\left[-\frac{r^2}{d^2\left(1+y^2\right)}\right]}{1+y^2}dy \qquad (22)$$

4. Evaluating the thermally affected zone

To study the thermic affected zone, the radial temperature distribution for extended irradiation periods is required. It results:

$$T(r)=T_a+\left(T_{1max}+T_{2max}\right)\cdot F_d(r) \qquad (23)$$

where $F_d(r)$ is:

$$F_d(r)=\frac{2}{\pi}\int_0^{\infty}\frac{\exp\left[-\frac{r^2}{d^2\left(1+y^2\right)}\right]}{1+y^2}dy \qquad (24)$$

representing "the correction function", derived from the condition of temperature distribution saturation during penetrating the material and for a certain laser beam focus.

To obtain values for $F_d(r)$, the improper integral relating a non-primitivable function (24) was transformed in an integral with finite limits, which was solved numerically.

By using the transform $y=\operatorname{tg}x$, the following expression was obtained:

$$F_d(r)=\frac{2}{\pi}\int_0^{\frac{\pi}{2}}\exp\left[-\left(\frac{r}{d}\right)^2\cos^2 x\right]dx \qquad (25)$$

$F_d(r)$ was computed for the following values of parameter $\bar{d}$: 0.16 mm, 0.200 mm, 0.238 mm, 0.25 mm, the interest domain of radial co-ordinate r being in the range 0.01...10 mm.

Taking into account the results obtained in the above mentioned points and by using the "Curve Expert" software, it was plotted the correction function $F_d(r)$ (fig. 1), and set up a regression function offering the best fitting with the plotted one.

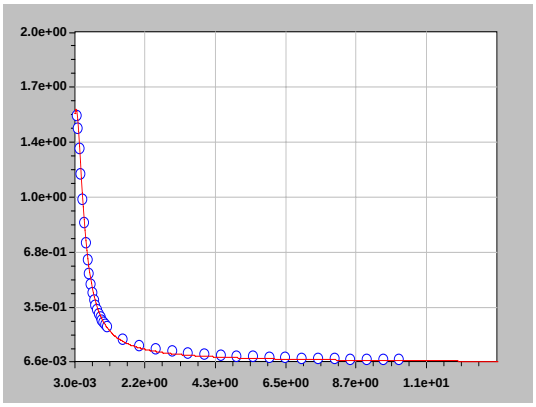

Fig. 1. Plotting the correction function $F_d(r)$.

The regression function is a rational one, having the following expression:

$$F_d(r) = \frac{2}{\pi} \cdot \frac{a + b \cdot r}{1 + c \cdot r + d \cdot r^2} \qquad (26)$$

The coefficients a, b, c values, function of $\bar{d}$ (the average radius of focused laser beam), are the following:

Table 1. Values of $F_d(r)$ function coefficients.

$\bar{d}$ [mm]	a	b	c	d
0.160	1.524	5.934	1.116	52.530
0.200	1.533	3.606	0.647	29.118
0.225	1.532	2.804	0.465	19.691
0.250	1.533	2.615	0.432	17.671

Figs. 2 and 3 are showing plots of temperature radial distribution respecting (23), for $\bar{d} = 0.25\text{mm}$, in case of steel processing. The results are within correct physical ranges.

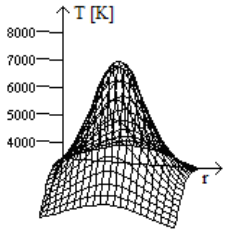

Fig. 2. Temperature radial distribution for x = y = 2mm.

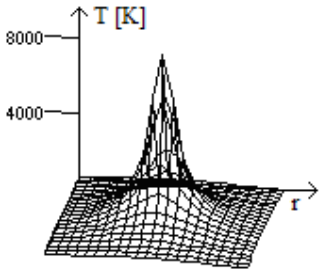

Fig. 3. Temperature radial distribution for x = y = 10mm.

It may be noticed the temperature maximum in the center of the interstice and a decreasing variation as the radial co-ordinate increases. The temperature reaches the vaporization and melting values at the interstice and respectively thermic affected zone limits.

The semi-interstice I is determined by using (23), choosing the temperature at the cut limit equal to vaporization temperature, T_{vap}.

It results:

$$T_{vap} = T_a + (T_{1max} + T_{2max}) F_d(I) \quad \Rightarrow \qquad (27)$$

$$T_{vap} = T_a + (T_{1max} + T_{2max}) \frac{2}{\pi} \int_0^{\infty} \frac{\exp\left[-\frac{I^2}{d^2(1+y^2)}\right]}{1+y^2} dy \qquad (28)$$

relation which allows the semi-interstice determination, the other quantities being known.

The thermally affected zone is approximated by the material domain of melting, followed by a solidifying. Relation (23) is used to compute the thermic affected zone (z_{IT}), by choosing the temperature at the limit of thermic affected zone equal to melting temperature T_{top}.

It results:

$$T_{top} = T_a + (T_{1max} + T_{2max}) F_d(I + z_{IT}) \quad \Rightarrow \qquad (29)$$

$$T_{top} = T_a + (T_{1max} + T_{2max}) \frac{2}{\pi} \int_0^{\infty} \frac{\exp\left[-\frac{(I+z_{IT})^2}{d^2(1+y^2)}\right]}{1+y^2} dy \qquad (30)$$

relation which allows thermally affected zone determination.

The cut width (2I), respectively thermic affected zone variations (z_{IT}) as functions of maximum temperature are presented in Figs. 4 and 5.

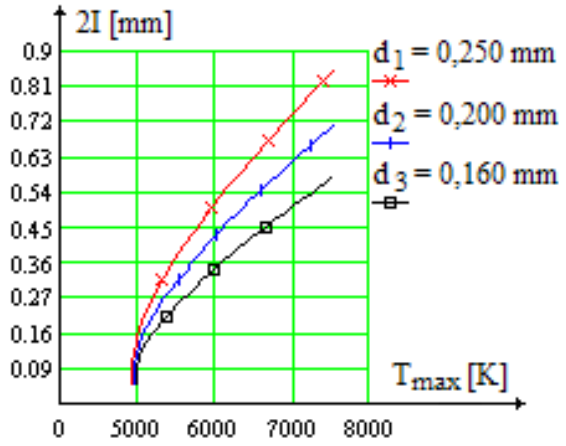

Fig.4. Cut width variation as function of maximum temperature.

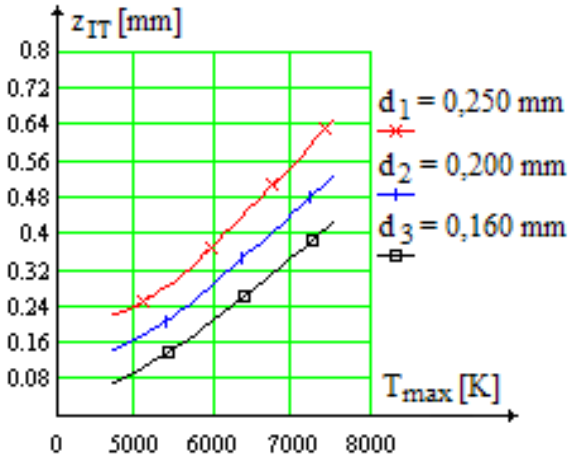

Fig.5. Thermally affected zone width variation as function of maximum temperature.

The following equations were solved to obtain the above mentioned plots:

$$\frac{a+b\cdot I}{1+c\cdot I+d\cdot I^2}=\frac{\pi}{2}\cdot\frac{T_{vap}-T_a}{T_{1\max}+T_{2\max}} \quad (31)$$

$$\frac{a+b(z_{IT}+I)}{1+c(z_{IT}+I)+d(z_{IT}+I)^2}=\frac{\pi}{2}\cdot\frac{T_{top}-T_a}{T_{1\max}+T_{2\max}} \quad (32)$$

choosing and plotting their positive solutions.

5. Experimental results

The thermic affected zone dimensions in case of metals processing may be determined by studying the material microhardness variation or measuring using a microscope the dimensions of zones in which the material suffered structural changes.

Materials used as probes were from plain steels (OL37) and blistered steels (21MoMnCr12) categories. The experiments to determine micro hardness variation of laser beam cut steels were fulfilled with EUROLAS 1502 laser installation, made by Messer Griesheim SchweiBtechnik and owned by S.C. Automecanica Moreni S.A. The installation includes a CO_2 laser from TRIAGON series (resonant cavity has triangularly geometry – three laser tubes laser triangular disposed), dc excited, with a power control range of 0÷3 kW.

Laser cuttings were experimented on above mentioned probes and micro hardness was measured in several points, both in thermally affected zone and in the core. It was studied the microhardness variation along the distance from the cutting edge inside the material surface, as well as the laser power influence on thermally affected zone microhardness.

Microhardness of the processed surfaces was measured with a Vickers micro-hardness-meter, type N32M30/5EZ, with a load of 100g, its holding time being 15s.

Figs. 6 and 7 are showing the imprints of the penetrater when measuring microhardness of the steels OL37 and 12Cr130.

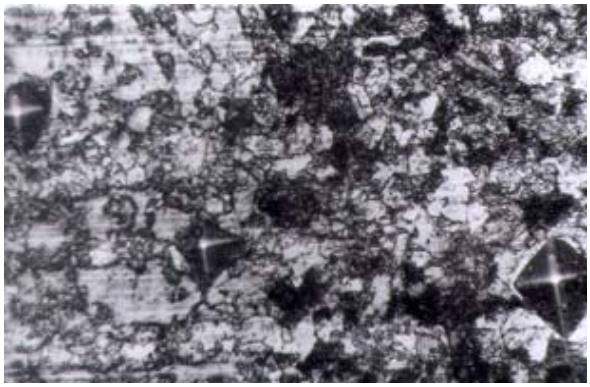

Fig. 6. Penetrater imprints for OL37.

Fig. 7. Penetrater imprints for 21MoMnCr12.

The experimental results are presented in Table 2.

Table 2. Experiments results, HV = f(x).

Nr. crt.	x [μm]	Microhardness [HV]		Nr. crt.	x [μm]	Microhardness [HV]	
		OL37	21MoMnCr12			OL37	21MoMnCr12
1	10	525	610	10	250	425	459
2	20	528	606	11	300	392	450
3	40	512	608	12	350	286	448
4	60	506	600	13	400	228	401
5	80	471	572	14	450	206	395
6	100	460	502	15	500	190	382
7	120	445	485	16	550	186	380
8	160	444	472	17	600	188	380
9	200	436	467	18	650	186	378

The origin of distance x is the cutting edge. The micro hardness variation (measured in Vickers units) along the distance x, the cutting speeds were 2500 mm/min (OL37) and 2000 mm/min (21MoMnCr12), with a laser power of 2000 W.

With the experimental results as input data, the software CurveExpert was used to obtain plots of micro hardness variation along the distance x (Fig. 8) for each processed material and to set up a regression function, which provides the best fitting with experimental data.

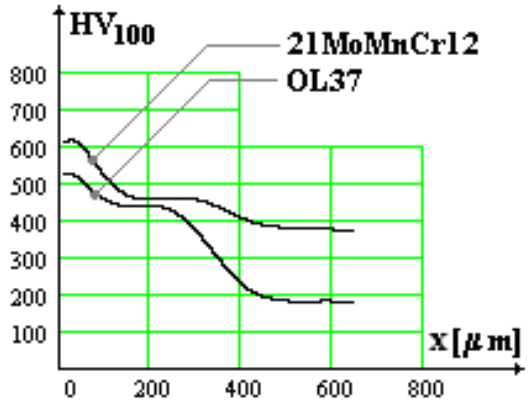

Fig.8. Micro hardness variation function of distance x.

The microhardness regression functions corresponding to a minimum standard error are polynomials of 7th degree.

Based on the experimental results, the following interest areas came out for the two probes studied:

- OL37: a hardened zone of aprox. 60μm, followed by a thermally affected zone of aprox. 360μm may be observed;
- 21MoMnCr12: a hardened zone of aprox. 90μm, followed by a thermally affected zone of aprox. 320μm may be observed.

Thermally affected zone width was determined by using (31) şi (32), the following laser and probes characteristics being taken into account as processing parameters:

$$g(21MoMnCr12) = 5mm;\ g(OL37) = 4mm;$$

$$P_L = 2000W;\ p_{O_2} = 3{,}2bar;\ d = 0{,}16mm.$$

Taking into account the processed materials parameters, the resulted width of thermic affected zones (z_{IT}) are the following:

$$z_{IT}(OL37) = 394\mu m;\quad z_{IT}(21MoMnCr12) = 381\mu m,$$

the error between theoretical and practical results being les than 10%.

6. Conclusions

The research objective was to study the laser effects towards the processed materials, the goal of this paper being to set up a rapid method for evaluating the thermally affected zone in case of processing metals with power laser beam assisted by an active gas jet. The paper desires to be a supplement in this research area, because only qualitative-intuitive information about causal link between the process parameters is available, so, experimental researches tend to determine their quantitative aspects. In technical literature only some approaches on theoretical and practical researches to determine gas assisted cutting process threshold values are available [2,11,12]. The mathematical models of cutting quality indicators are missing too, the theoretical and experimental researches focussing to solve this problem. The main advantage of the proponed method is its easiness to be applied, the thermally affected zone being achieved by solving (31) and (32). Constants a, b, c and d were determined considering 4 frequent values of the focused laser beam diameter.

The presented equations came out from the heating equation solutions, applied to a semi-infinite solid with a "Gaussian" distributed energy flow. The main equation of this approach is the correction function (24), allowing the radial temperature distribution computing.

It may be noticed that the correction function $F_d(r)$ depends only of focalization $\bar{d}$ of the focusing system, while the maximum temperature, T_{max}, achievable in the center of the interstice, depends of processing parameters totality (laser system, focusing system, assisting gas, processed material, processing installation).

According to experiments, the thermally affected zone may be assumed as the same with the zone of steel decarburization, the theoretical results being confirmed by the practical ones.

It may be observed that material micro hardness generally has two discontinuities: the first at hardening zone limit, and the second at thermally affected zone limit. High chrome concentration steels present a melting zone too, with a lower micro hardness value.

Materialmicro hardness, as well as the thermally affected zone dimensions, increasingly depends on laser beam power, owing the temperature increasing in working zone. The results thus obtained are within the limits of

normal physics, which constitutes a verifying of the mathematical model equation.

Acknowledgements

This research work is supported by The National Authority for Scientific Research (CNCSIS Romania): Grant CNCSIS, PN-II-ID-PCE-2008, code 2291: "Laser Radiation-Substance Interaction: Physical Phenomena, Modelling and Techniques of Electromagnetic Pollution Rejection".

References

[1] F. Bachmann, Proceedings of SPIE – The International Society of Optical Engineering **6735**, art. no. 67350T, 2007.
[2] I. Belic, Optics and Laser Technology **40**(4), 277 (2008).
[3] V. Draganescu, V. G. Velculescu, Thermal Cutting With Laser Beams, Academy Publishing House, Bucharest, 1986.
[4] J. M. Dowden, The Mathematics of Thermal Modelling, Chapman & Hall/CRC, 2001.
[5] J. M. Dowden, The Theory of Laser Materials Processing, Published by Springer, 29, 2008.
[6] N. Jebbari, M. M. Jebari, F. Saadallah, A. Tarrats-Saugnac, J. P. Longuemard, Optics and Laser Technology, November 2007.
[7] M. Pearsica, I.G. Ratiu, C. G. Carstea, C. Constantinescu, C. Strimbu, L. Gherman, WSEAS Transactions on Mathematics **7**(11), 2174 (2008).
[8] M. Pearsica, I. G. Ratiu, C. G. Carstea, C. Constantinescu, C. Strimbu, Proceedings of the 10th WSEAS Int. Conf. on Mathematical Methods, Computational Technique and Intelligent Systems, Corfu, Greece, October 2008.
[9] M. Pearsica, S. Nedelcu, Int. Conf. – Applied Electronics, Pilsen, Cehia, September, 269 (2005).
[10] J. Perriere, E. Milton, E. Fogarassy, Recent Advaces in Laser Processing Materials, Published by Elsevier, 2006.
[11] J. F. Ready, LIA Handbook of Laser Materials Processing, Laser Institute of America Magnolia Publishing, Inc., 437, 2001.
[12] S. Z. Shuja, B. S. Yilbas, S. M. Khan, Optics and Laser Technology **40**(3), 472 (2008).
[13] W. M. Steen, Laser Material Processing, Published by Springer, 2003.

*Corresponding author: marianpearsica@yahoo.com